

Capillary condensation in one-dimensional irregular confinement

Thomas P. Handford,¹ Francisco J. Pérez-Reche,² and Sergei N. Taraskin³

¹*Department of Chemistry, University of Cambridge, Cambridge, UK**

²*Institute for Complex Systems and Mathematical Biology,
King's College, University of Aberdeen, Aberdeen, UK[†]*

³*St. Catharine's College and Department of Chemistry, University of Cambridge, Cambridge, UK[‡]*

A lattice-gas model with heterogeneity is developed for the description of fluid condensation in finite sized one-dimensional pores of arbitrary shape. An exact solution of the model is presented that reproduces the experimentally observed dependence of the amount of fluid adsorbed in the pore on external pressure. The proposed framework is viewed as a fundamental building block of the theory of capillary condensation necessary for reliable structural analysis of complex porous media from adsorption-desorption data.

PACS numbers: 75.10.Nr, 05.70.Np, 68.43.-h, 64.70.F-

Physical systems which consist of networks of pores, such as Vycor [1], Silica aerogels [2], porous rocks [3], soil [4] and others, have a wide spectrum of applications, ranging from molecular filters and catalysts [5] to fuel storage [6]. Capillary condensation is an important and interesting physical phenomenon occurring in many such systems. In recent years, a lot of experimental and theoretical work has been undertaken in order to understand the link between the structure of porous materials and capillary condensation [2, 7, 8]. However, recent works suggest that understanding of capillary condensation is still poor [8]. The situation is critical since routinely used classical theories fail to explain experimental observations [9] of capillary condensation even in simple one-dimensional (1D) isolated pores. In particular, classical theories have failed to explain the way in which the amount of adsorbed fluid varies as pressure increases and decreases, i.e. the appearance and form of hysteresis in sorption curves [10, 11]. For example, according to classical theories, pores closed at one end should not have hysteresis, which is in contradiction to existing experimental data [10]. An accurate theory for capillary condensation in 1D pores is ultimately necessary to ensure that, for instance, this phenomenon can be used as a reliable technique to probe the structure of generic porous media consisting of a network of interlinked 1D pores [12].

A possible theoretical explanation of these phenomena is that the appearance of hysteresis is caused by heterogeneity of the pores, which includes variable pore diameter, chemical heterogeneity in the pore walls and roughness of internal surfaces [13–16]. Numerical analyses such as lattice based mean-field theory [17] and multi-scale molecular dynamics studies [18, 19] have given numerical support to this explanation. Additionally, these numerical approaches have revealed the occurrence of avalanches (sudden jumps) in the amount of adsorbed fluid during condensation and evaporation. Such avalanches bare similarity to avalanches in magnetisation found in the zero-temperature random-field Ising model (zt-RFIM) [20, 21]. Employing this similarity, we map

zt-RFIM to the lattice-gas model and demonstrate that: (i) a heterogeneous lattice-gas model is a minimally sufficient model to reproduce experimental observations in finite-sized pores; (ii) this model can be solved exactly analytically by a novel technique, with the solution being fully supported by numerical results; (iii) such an analytical solution leads to simple physical explanations and interpretations of experimental results and predicts the shape of sorption curves for unexplored regimes. More specifically, we demonstrate that (i) the effects of the closed and open ends of the pores, considered important in the classical theories, are significantly reduced for large disorder in strengths of the interactions of the fluid with the pore walls; (ii) a positive-skewed distribution in strengths of such interactions can lead to sorption curves of the same form as those found experimentally [10, 11]; (iii) in cylindrical pores consisting of two parts of different diameter, condensation and evaporation in one part can induce condensation and evaporation in the rest of the pore for low disorder, but for high disorder, the two parts of the pore behave independently.

The analyzed model is based on a standard lattice-gas model of capillary condensation [2, 9, 21]. In this model, the 3D space is split into cells, and each cell can be filled either by matrix (the solid substrate), fluid or vapour. If the cell i is occupied by matrix (expressed by setting parameter $\eta_i = 0$), then it cannot become occupied by fluid or vapour. It is assumed that the variables η_i are quenched for the whole system and thus the matrix state cannot change during the condensation. If cell i is not occupied by the matrix ($\eta_i = 1$), then it can be occupied by either fluid ($\tau_i = 1$) or vapour ($\tau_i = 0$). The variables τ_i can vary with the change in chemical potential, μ . The Hamiltonian which describes the lattice gas model is given by [21],

$$\mathcal{H} = -\mu \sum_i \tau_i \eta_i - w^{\text{ff}} \sum_{\langle ij \rangle} \tau_i \tau_j \eta_i \eta_j - \sum_{\langle ij \rangle} [\tau_i w_{ij}^{\text{mf}} \eta_i (1 - \eta_j) + \tau_j w_{ji}^{\text{mf}} \eta_j (1 - \eta_i)] \quad (1)$$

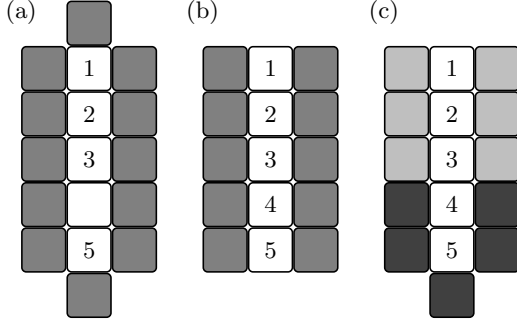


FIG. 1. Diagram showing 2D sections of (a) a linear pore of $N = 5$ cells unoccupied by matrix, labelled $i = 1, \dots, 5$ (white squares), and surrounded by matrix cells (grey squares) in the 3D system, (b) a linear pore with open ends and (c) a linear pore of $N = 5$ cells with one open and one closed end consisting of two sections represented by light- and dark-grey cells. The interaction of the fluid in cells $1 \leq i \leq N_1 = 3$ and in cells $4 < i \leq N$ with the matrix represented by light-grey and dark-grey squares is described by $\langle w_1^{\text{mf}} \rangle$, and $\langle w_2^{\text{mf}} \rangle$, respectively. For clarity, 2 relevant matrix cells per unoccupied cell, on top of and underneath the white cells, are not shown in this 2D diagram.

where the summations run over all the cells in the system in the first term and over all nearest-neighbour pairs $\langle ij \rangle$ in the other terms. The fluid-fluid interaction parameter, $w^{\text{ff}} > 0$, is assumed to be the same for all pairs of cells. The matrix-fluid interaction strength between the matrix at cell j and fluid at the neighbouring cell i is described by the parameter w_{ij}^{mf} . The values of w_{ij}^{mf} are considered to be independently distributed quenched random variables with the probability density function, $\rho_i(w_{ij}^{\text{mf}})$, which can be cell dependent. The random distribution of this parameter has been studied previously in the context of chemical heterogeneity of the pore walls [22], but below it is assumed to characterise all types of heterogeneity. For concreteness, we focus on two forms of disorder in w_{ij}^{mf} , representing heterogeneity on different scales ranging from local fluctuations at a single point on the pore wall to a variable diameter of the pore: (i) a normal distribution, $\rho_i(w_{ij}^{\text{mf}}) = \mathcal{N}(\langle w^{\text{mf}} \rangle_i, \Delta_i^2)$ and (ii) an exponential distribution with correlations ensuring that all w_{ij}^{mf} are the same for the same cell i , and distributed according to, $\rho_i(w_{ij}^{\text{mf}}) = \Theta(x) \Delta_i^{-1} \exp(-\Delta_i^{-1} x)$ (where $x = (w_{ij}^{\text{mf}} - \langle w^{\text{mf}} \rangle_i) + \Delta_i$ and $\Theta(x)$ is the Heaviside step function), with mean $\langle w^{\text{mf}} \rangle_i$ and variance Δ_i^2 . Thermal fluctuations are ignored, under the assumption that the temperature is much smaller than all typical energy scales in the problem, $T \ll w^{\text{ff}}, \langle w^{\text{mf}} \rangle_i$.

The Hamiltonian described by Eq. (1) can be mapped onto the Hamiltonian for the zt-RFIM [21], i.e. $\mathcal{H} = -J \sum_{\langle ij \rangle} s_i s_j - \sum_i h_i s_i - H \sum_i s_i$, where the variable $s_i = (2\tau_i - 1)\eta_i$ ($s_i = \pm 1$) represents a spin state, $H = \mu/2$ refers to an external magnetic field, and $J = w^{\text{ff}}/4$

describes the spin-spin interaction. The random fields h_i at cell i are given by $h_i = \sum_{j/i} ((1 - \eta_j)w_{ij}^{\text{mf}}/2 + \eta_j w^{\text{ff}}/4)$ with the sum running over all nearest neighbours of i . We study the zt-RFIM with cell-dependent random-field distributions. These distributions depend on the pore geometry chosen. Several forms of 1D pore geometries embedded in a simple cubic lattice are analysed: linear pores (i) with closed ends (see Fig. 1(a)), (ii) with open ends bounded by vapour (see Fig. 1(b)), and (iii) with one open end and one closed end. In the last case, we consider two distinct sections of lengths N_1 and $N - N_1$ characterised by different values of mean matrix-fluid interaction $\langle w_1^{\text{mf}} \rangle$ and $\langle w_2^{\text{mf}} \rangle$, respectively (see Fig. 1(c)), intended to model ink-bottle and funnel geometries, with weaker matrix-fluid interaction representing a larger diameter. The random field, h_i , at cell i is characterised by a distribution, $\rho_{h_i}(h_i)$, which depends on the numbers, $n_i^{\text{m}} = \sum_{j/i} (1 - \eta_j)$ and $n_i^{\text{u}} = \sum_{j/i} \eta_j$, of neighbouring cells which are occupied and unoccupied by matrix, respectively. When w_{ij}^{mf} is normally distributed, the random field at cell i is distributed according to $\rho_{h_i}(h_i) = \mathcal{N}(\langle h_i \rangle_i, \Delta_{h_i}^2)$ with $\langle h_i \rangle_i = (n_i^{\text{m}}/2)\langle w^{\text{mf}} \rangle_i + (n_i^{\text{u}}/4)w^{\text{ff}}$ and $\Delta_{h_i}^2 = (n_i^{\text{m}}/2)\Delta_i^2$. When w_{ij}^{mf} follows a correlated exponential distribution, the random field at cell i is distributed according to $\rho_{h_i}(h_i) = \Theta(y) \Delta_{h_i}^{-1} \exp(-\Delta_{h_i}^{-1} y)$ (where $y = h_i - \langle h_i \rangle_i + \Delta_{h_i}$), with the mean $\langle h_i \rangle_i$ being the same as for the normal distribution and standard deviation $\Delta_{h_i} = n_i^{\text{m}} \Delta_i / 2$. According to the dynamical rules of the zt-RFIM, for adsorption (desorption) each cell is initially empty (occupied), $s_i = -1$ ($s_i = +1$), and can become occupied by fluid (empty), $s_i = +1$ ($s_i = -1$), once its local field, $f_i = h_i + H + J \sum_{j/i} s_j$, is positive, $f_i > 0$ (negative, $f_i < 0$).

In order to find sorption curves for a 1D pore, we develop a novel method based on the use of the generating function formalism [23, 24]. Within this formalism, the volume of fluid in the finite pore is a random value and can be expressed by a generating function, $G(x) = \sum_{n=0}^N P(n)x^n$, where $P(n)$ is the probability that $n = \sum_{i=1}^N \tau_i$ cells in the finite chain are occupied by fluid. The mean volume of fluid is given by

$$\langle V \rangle = V_0 \langle n \rangle = \partial_x G(1), \quad (2)$$

with volume of a cell set to $V_0 = 1$, and the variance is,

$$\text{Var}[V] = \partial_{xx} G(1) + \partial_x G(1) - [\partial_x G(1)]^2, \quad (3)$$

where $\partial_x G(1)$ and $\partial_{xx} G(1)$ refer to the first and second derivatives of $G(x)$ with respect to x evaluated at $x = 1$.

Based on the recursive relaxation scheme used in Ref. [25], an exact expression for the generating function $G(x)$ can be derived (see [26] for technical details),

$$G(x) = [\mathbf{A}(x)]^T \mathbf{M}_{N-1}(x) \mathbf{M}_{N-2}(x) \dots \mathbf{M}_2(x) [\mathbf{B}(x)] \quad (4)$$

where,

$$[\mathbf{A}(x)]^T = (xp'_{N,1} + (1 - p'_{N,1}), xp'_{N,0}, 1 - p'_{N,0}) ,$$

$$\mathbf{M}_i(x) = \begin{pmatrix} xp_{i,1} & xp_{i,0} & 0 \\ x(p_{i,2} - p_{i,1}) + (1 - p_{i,2}) & x(p_{i,1} - p_{i,0}) & 1 - p_{i,1} \\ 1 - p_{i,1} & 0 & 1 - p_{i,0} \end{pmatrix} ,$$

$$[\mathbf{B}(x)]^T = (xp'_{1,0}, x(p'_{1,1} - p'_{1,0}) + 1 - p'_{1,1}, 1 - p'_{1,0})(5)$$

Here, the values of $p'_{i,m} = \tilde{p}_{i,m}^{(1)}$ ($i = 1, N$) and $p_{i,m} = \tilde{p}_{i,m}^{(2)}$ ($1 < i < N$) are the probabilities that cell i , with m occupied neighbouring cells, has a positive local field, which are given by $\tilde{p}_{i,m}^{(k)} = \int_{h=-H-J(2m-k)}^{\infty} \rho_{h_i}(h)dh$. Eq. (4) is the main analytical result of our analysis allowing exact evaluation of $\partial_x G(1)$ and $\partial_{xx} G(1)$. The mean and variance of the volume of fluid in the pore can be found for both adsorption and desorption regimes using Eqs. (2) and (3) along with the derivatives of $G(x)$. Technically, the derivatives of $G(x)$ can be calculated by numerical iteration, i.e. the derivatives of $\mathbf{M}_i(x)\mathbf{M}_{i-1}(x) \dots \mathbf{M}_2(x)\mathbf{B}(x)$ can be found in terms of the derivatives of $\mathbf{M}_{i-1}(x) \dots \mathbf{M}_2(x)\mathbf{B}(x)$.

The analysis presented below is based on the numerical solution for $G(x)$ given by Eq. (4) and supported by Monte-Carlo simulations of condensation in a pore within the framework of the lattice-gas model. During each simulation, the value of μ was fixed, and hysteresis plots were obtained by running separate simulations for each value of μ . The fluid occupation number of the matrix-free cells was changed following single spin-flip zero-temperature Glauber dynamics [20, 27]. The mean and variance of V were calculated by averaging over 10^4 realisations of the disorder in random-fields for a fixed matrix structure and values of the parameters. Figs. 2 and 3 show that the agreement between analytical calculations (lines) and numerical simulations (symbols) is excellent.

Our first result is that, for low disorder in w^{mf} , adsorption in finite open-ended pores occurs in a single avalanche. This is evident from the fact that the variance reaches almost the maximum value $\text{Var}[V]_{\text{max}} = 0.25$ (see right dashed peak in the lower panel of Figs. 2(a)) implying that the system is either fully occupied or fully unoccupied and there are no intermediate stable states (no pinning points). In contrast, for pores with closed ends, adsorption occurs at a lower value of μ (compare right hand solid and dashed curves in upper panel of Figs. 2(a)) with the propagation of a meniscus between several pinning points in a number of separate avalanches, indicated by a lower $\text{Var}[V]$ (see right solid peaks in the lower panel of Figs. 2(a)). The reason for this is that one of the cells at the ends of the closed-ended pores is occupied first with high probability, thus nucleating the adsorption process in the form of meniscus propagation. For the open-ended pore, no cell can become occupied until

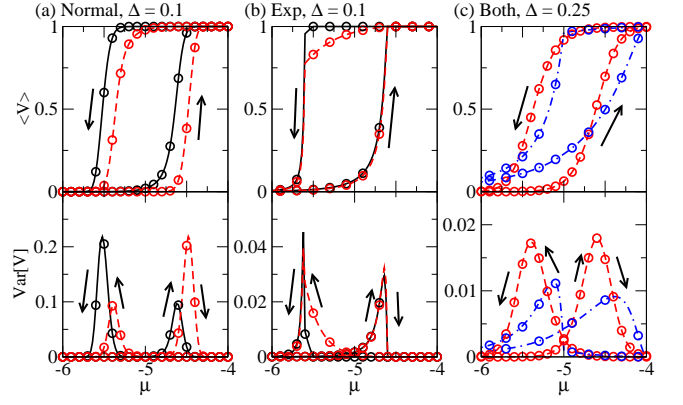


FIG. 2. The mean $\langle V \rangle$ (upper panel) and variance $\text{Var}[V]$ (lower panel) of occupied volume of linear pores with length $N = 100$ is plotted vs μ . The arrows show the direction in which μ changes for adsorption and desorption curves. The solid (dashed and dot-dashed) curves correspond to pores with closed (open) ends. Different columns refer to different types and degrees of disorder in w_{ij}^{mf} with the same mean value $\langle w^{\text{mf}} \rangle = 1.0$ and the same $w^{\text{ff}} = 1.0$: (a) $\rho(w^{\text{mf}})$ is normal with width $\Delta = 0.1$; (b) correlated exponential distribution with dispersion $\Delta = 0.1$ (c) normal (dashed) and correlated exponential (dot-dashed) with width $\Delta = 0.25$. Symbols refer to the numerical results.

a much higher value of μ is reached, so that there are no pinning points at which the propagation of meniscus can stop and the avalanche, initiated at any cell in the pore, proceeds along the whole pore in one step. For desorption, the situation is reversed to that for adsorption, with nucleation (evaporation) occurring at the end-point cells $i = 1, N$ in the open-ended pores first. At high disorder, both adsorption and desorption in all geometries shown in Fig. 1 occur mainly via many small avalanches (indicated by a low variance in the lower panels of Fig. 2(c)). The sorption curves for open and closed ended pores are identical, agreeing with numerical results [17] found for pores with both ends open or one end open. This is because there are some cells with high w^{mf} which nucleate the adsorption and pin the desorption and some cells with low w^{mf} which pin the adsorption and nucleate the desorption.

Our second result is that the correlated exponential distribution of disorder in w^{mf} can result in a so-called H2-type hysteresis [28] (see upper panel of Fig. 2(b) and dot-dashed lines in upper panel of (c)). This effect can be attributed to asymmetry in the distribution of random fields h_i , because a symmetric distribution will lead to a symmetric hysteresis loop, due to the symmetry of the Hamiltonian of the zt-RFIM. The asymmetry in the distribution of $h_i = \sum_{j/i} w_{ij}^{\text{mf}}$ can be achieved by a correlated asymmetric distribution of w_{ij}^{mf} . Indeed, if w_{ij}^{mf} are uncorrelated for a given value of i then the central limit theorem ensures that their sum is approximately distributed according to a normal (symmetric) distribu-

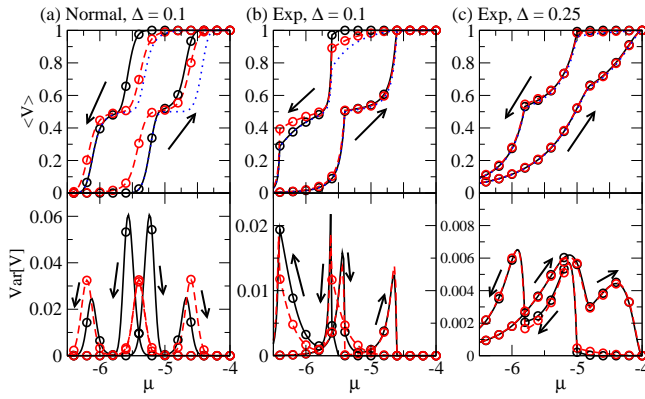


FIG. 3. $\langle V \rangle$ (upper panel) and $\text{Var}[V]$ (lower panel) for the linear pores shown in Fig. 1(c) of length $N = 100$ vs μ . The curves of different styles refer to different geometries, i.e. ink-bottle (solid lines), with $N_1 = 50$, $w_1 = 1.2$, $w_2 = 1.0$ and funnel (dashed lines), with $N_1 = 50$, $w_1 = 1.0$, $w_2 = 1.2$. The light dotted lines in the upper panels of (a)-(c) correspond to the mean occupied volume of two separate open-ended pores (shape (b) in Fig. 1) of length $N = 50$ one of which having $\langle w_{ij}^{\text{mf}} \rangle = 1.0$ for all cells and the other having $\langle w_{ij}^{\text{mf}} \rangle = 1.2$ for all cells. In (c), the solid, dashed and dotted lines coincide on the scale of the graph. In all cases, $w^{\text{ff}} = 1.0$. Each column represents a different degree or form of disorder: (a) normally distributed, $\Delta = 0.1$ (b) correlated exponentially distributed, $\Delta = 0.1$ and (c) correlated exponentially distributed, $\Delta = 0.25$. Arrows show the direction of change of μ for adsorption and desorption and symbols refer to numerical data.

tion. Therefore correlations in w_{ij}^{mf} play a significant role in achieving a skewed distribution of h_i and H2-type hysteresis, the effect being maximal when they are fully correlated, i.e. when all w_{ij}^{mf} are equal for a given i . This implies that H2-type hysteresis in heterogeneous pores arises due to variations in pore diameter (represented by correlated disorder in w_{ij}^{mf}) rather than due to individual defects, in agreement with previous numerical studies [17]. On the other hand, symmetric (normal) disorder in local fields (i.e. uncorrelated disorder in w_{ij}^{mf}) can only cause a parallel sided H1-type hysteresis, and may represent defects on small scales (Fig. 2(a)).

Our third result refers to an explanation of the experimental observations of condensation in pores with ink-bottle and funnel geometries. In pores consisting of two connected cylindrical sections of different diameters and a rough surfaces, it has been observed [11] that the condensation of fluid in the two parts of the pore occurs independently and is unaffected by which end of the pore is open. We have found that a similar effect occurs for the ink-bottle shape (see Fig. 1(c)) where the sections with different values w_1^{mf} and w_2^{mf} represent sections of different diameter used in experiments. Indeed, in Fig. 3(c) the adsorption-desorption curves are shown for large, correlated disorder in w_{ij}^{mf} . The resulting curves are identical to those found by adding together the adsorption-desorption curves for the two isolated halves of the

ink-bottle pore. For completeness, we also present the adsorption-desorption curves for small degrees of uncorrelated (Fig. 3(a)) and asymmetric correlated (Fig. 3(b)) disorder in w_{ij}^{mf} . In this case, there are significant interactions between the two sections, meaning that adsorption and desorption occur in the wider section at a higher value of μ in the funnel geometry (dashed lines in Fig. 3(a)-(b)) than in the ink-bottle geometry (solid lines in Fig. 3(a)-(b)).

To conclude, a heterogeneous lattice-gas model has been proposed to describe fluid condensation in 1D pores of different shapes and rough surfaces. Heterogeneity is the key and sufficient feature of the model which allows it to reproduce the main experimental findings. In physical systems exhibiting a more complex topology, e.g. a 3D maze-like network of 1D channels, an analytical solution may be nontrivial, however numerical simulations within this model can be performed straightforwardly for porous media of arbitrary topology.

TPH acknowledges the support of EPSRC.

* tph32@cam.ac.uk

† fperez-reche@abdn.ac.uk

‡ snt1000@cam.ac.uk

- [1] H.-J. Woo and P. A. Monson, Phys. Rev. E **67**, 041207 (Apr 2003)
- [2] L. D. Gelb, K. E. Gubbins, R. Radhakrishnan, and M. Sliwinski-Bartkowiak, Reports on Progress in Physics **62**, 1573 (1999), <http://stacks.iop.org/0034-4885/62/i=12/a=201>
- [3] D. Broseta, L. Barré, O. Vizika, N. Shahidzadeh, J.-P. Guilbaud, and S. Lyonard, Phys. Rev. Lett. **86**, 5313 (Jun 2001), <http://link.aps.org/doi/10.1103/PhysRevLett.86.5313>
- [4] F. J. Pérez-Reche, S. N. Taraskin, W. Otten, M. P. Viana, L. d. F. Costa, and C. A. Gilligan, Phys. Rev. Lett. **109**, 098102 (Aug 2012), <http://link.aps.org/doi/10.1103/PhysRevLett.109.098102>
- [5] P. I. Ravikovitch, D. Wei, W. T. Chueh, G. L. Haller, and A. V. Neimark, The Journal of Physical Chemistry B **101**, 3671 (1997)
- [6] M. Felderhoff, C. Weidenthaler, R. von Helmolt, and U. Eberle, Phys. Chem. Chem. Phys. **9**, 2643 (2007), <http://dx.doi.org/10.1039/B701563C>
- [7] R. Valiullin, J. Karger, and R. Glaser, Phys. Chem. Chem. Phys. **11**, 2833 (2009), <http://dx.doi.org/10.1039/B822939B>
- [8] P. Monson, Microporous and Mesoporous Materials **160**, 47 (2012), ISSN 1387-1811
- [9] R. Evans, Journal of Physics: Condensed Matter **2**, 8989 (1990), <http://stacks.iop.org/0953-8984/2/i=46/a=001>
- [10] B. Coasne, A. Grosman, N. Dupont-Pavlovsky, C. Ortega, and M. Simon, Phys. Chem. Chem. Phys. **3**, 1196 (2001), <http://dx.doi.org/10.1039/B009105G>
- [11] D. Wallacher, N. Künzner, D. Kovalev, N. Knorr, and K. Knorr, Phys. Rev. Lett. **92**, 195704 (May 2004)
- [12] Y. C. Yortsos, “Methods in the physics of porous media,”

- (Academic Press, San Diego, 1999) Chap. 3, p. 69
- [13] M. W. Maddox, J. P. Olivier, and K. E. Gubbins, *Langmuir* **13**, 1737 (1997)
 - [14] K. J. Edler, P. A. Reynolds, and J. W. White, *The Journal of Physical Chemistry B* **102**, 3676 (1998)
 - [15] V. Fenelonov, A. Derevyankin, S. Kirik, L. Solovyov, A. Shmakov, J.-L. Bonardet, A. Gedeon, and V. Romannikov, *Microporous and Mesoporous Materials* **44-45**, 33 (2001), ISSN 1387-1811, <http://www.sciencedirect.com/science/article/pii/S138718110000164>
 - [16] C. G. Sonwane, C. W. Jones, and P. J. Ludovice, *The Journal of Physical Chemistry B* **109**, 23395 (2005)
 - [17] S. Naumov, A. Khokhlov, R. Valiullin, J. Kärger, and P. A. Monson, *Phys. Rev. E* **78**, 060601 (Dec 2008)
 - [18] J. Puibasset, *The Journal of Chemical Physics* **127**, 154701 (2007)
 - [19] J. Puibasset, *Langmuir* **25**, 903 (2009)
 - [20] J. P. Sethna, K. Dahmen, S. Kartha, J. A. Krumhansl, B. W. Roberts, and J. D. Shore, *Phys. Rev. Lett.* **70**, 3347 (May 1993), <http://link.aps.org/doi/10.1103/PhysRevLett.70.3347>
 - [21] E. Kierlik, M. L. Rosinberg, G. Tarjus, and E. Pitard, *Molecular Physics* **95**, 341 (1998)
 - [22] S. Naumov, R. Valiullin, J. Kärger, and P. A. Monson, *Phys. Rev. E* **80**, 031607 (Sep 2009)
 - [23] M. E. Fisher and J. W. Essam, *Journal of Mathematical Physics* **2**, 609 (1961), <http://link.aip.org/link/?JMP/2/609/1>
 - [24] S. Sabhapandit, P. Shukla, and D. Dhar, *Journal of Statistical Physics* **98**, 103 (2000), ISSN 0022-4715, 10.1023/A:1018622805347
 - [25] D. Dhar, P. Shukla, and J. P. Sethna, *Journal of Mathematical and General* **30**, 5259 (1997), <http://stacks.iop.org/0305-4470/30/i=15/a=013>
 - [26] see supplemental material at <http://link.aps.org/supplemental/xxxx> for details.
 - [27] T. P. Handford, F.-J. Perez-Reche, and S. N. Taraskin, *Journal of Statistical Mechanics: Theory and Experiment* **2012**, P01001 (2012), <http://stacks.iop.org/1742-5468/2012/i=01/a=P01001>
 - [28] K. S. W. Sing, D. H. Everett, R. A. W. Haul, L. Moscou, R. A. Pierotti, J. Rouquerol, and T. Siemieniowska, *Pure and Applied Chemistry* **57**, 603 (1985), ISSN 0033-4545, <http://dx.doi.org/10.1351/pac198557040603>

Supplementary Note

Thomas P. Handford¹, Francisco J. Pérez-Reche², and Sergei N. Taraskin³

¹Department of Chemistry, University of Cambridge, Cambridge, UK

²Institute for Complex Systems and Mathematical Biology, King's College, University of Aberdeen, Aberdeen, UK

³St. Catharine's College and Department of Chemistry, University of Cambridge, Cambridge, UK

In this supplementary note, we derive an exact expression for the mean and variance of the volume occupied by fluid in a 1D pore consisting of N cells. This is done by establishing a recursion relation for the generating function,

$$G(x) = \sum_{n=0}^N P(n)x^n, \quad (1)$$

for the probability, $P(n)$, that n of the cells in the pore are occupied by fluid. The abelian property of the zt-RFIM means that the final state of the system is independent of the order in which the cells are occupied by fluid (the order spins flip) as long as the system ends up in a stable or metastable state [1, 2]. Therefore, we use particular dynamical rules for occupancy of cells that are convenient from a mathematical viewpoint. Assume that the relaxation of the system into a metastable state takes place in a series of N time-steps, t , $1 \leq t \leq N$. Initially, during time-step $t = 1$, all the cells with $i \geq 2$ are artificially prevented from being occupied, while the first cell $i = 1$ is allowed to change its state. Cell $i = 1$ can either change state from unoccupied to occupied if the local field is positive $f_i > 0$, or remain unoccupied if the local field is negative. This process with two possible outcomes is called relaxation of cell 1. Next, during time-step $t = 2$, we allow cell $i = 2$ to relax, while cells $i \geq 3$ are still held in the unoccupied state, and cell $i = 2$ can become occupied if $f_2 > 0$. If cell $i = 2$ does become occupied, then the local field f_1 at cell $i = 1$ will increase. This can cause cell $i = 1$ to become occupied if it was not occupied already, i.e. an avalanche can pass from cell $i = 2$ to cell $i = 1$ during time-step $t = 2$. Similarly, we then allow the next cell in the chain, i.e. $i = 3$, to relax and if it becomes occupied an avalanche can pass back along the pore towards cell $i = 1$ if those cells with $i < 3$ were not occupied. This method is recursively applied until all the cells in the system are relaxed, after time-step $t = N$.

Let us consider the cell $i = N$ at the end of the pore, which is the last cell to be allowed to relax in the above procedure. At the start of time-step $t = N$, the neighbouring pore cell $i = N - 1$ can be occupied or unoccupied, i.e. $s_{N-1} = \pm 1$. If the neighbouring cell $i = N - 1$ is occupied ($s_{N-1} = +1$), and the random field at cell $i = N$ is $h_N > -J - H$, then the local field $f_N > 0$ and cell $i = N$ will become occupied. This occurs with cell-dependent probability $p'_{N,1}$ where,

$$p'_{i,m} = \int_{h_i = -H - J(2m-1)}^{\infty} \rho_{\text{RF},i}(h_i) dh_i, \quad (2)$$

with m being the number of occupied neighbours of cell $i = N$, i.e. $m = 1$ in this case. If, however, the neighbouring cell $i = N - 1$ is unoccupied ($s_{N-1} = -1$), then the local random field must be above a higher threshold for cell N to become occupied, $h_N > J - H$, which occurs with probability, $p'_{N,0}$, given by Eq. (2) with $m = 0$. In this case, the field at cell $i = N - 1$ will increase, and an avalanche can propagate back along the pore.

The probability that there are n occupied cells in the lattice at the end of the relaxation process can therefore be written as,

$$\begin{aligned} P(n) = & P_A(N-1, n-1)p'_{N,1} + P_A(N-1, n)(1 - p'_{N,1}) \\ & + P_B(N-1, n-1)p'_{N,0} + P_C(N-1, n)(1 - p'_{N,0}), \end{aligned} \quad (3)$$

in terms of the probabilities, $P_A(i, n')$, $P_B(i, n')$ and $P_C(i, n')$, which can be recursively determined. The quantity,

$$P_A(i, n') = \text{Prob}[n_i(t=i) = n' \cap s_i(t=i) = +1], \quad (4)$$

is the probability that at the end of time-step $t = i$, there are $n_i(t=i) = n'$ occupied cells j in the range $1 \leq j \leq i$ (i.e. $n_i = \sum_{j=1}^i (s_j + 1)/2$) and that cell i is occupied, $s_i(t=i) = +1$. The value,

$$P_B(i, n') = \text{Prob}[s_i(t=i) = -1 \cap n_i(t=N) = n' | s_{i+1}(t=N) = +1], \quad (5)$$

is the probability that cell i is unoccupied at end of time-step $t = i$, $s_i(t = i) = -1$, and at the end of the relaxation process (end of time-step $t = N$) there are $n_i = n'$ occupied cells in the range $1 \leq j \leq i$, given that cell $i + 1$ becomes occupied, $s_{i+1}(t = N) = +1$, during some time-step t' , $i < t' \leq N$ (which causes avalanches to pass back along the chain towards cell 1, changing the occupation number n_i). The third quantity,

$$P_C(i, n') = \text{Prob}[n_i(t = i) = n' \cap s_i(t = i) = -1] , \quad (6)$$

is the probability that at the end of time-step $t = i$ there are $n_i(t = i) = n'$ occupied cells in the range $1 \leq j \leq i$ and that cell i is unoccupied at this time-step, $s_i(t = i) = -1$. Using Eq. (3), the generating function $G(x)$ for the total number of occupied cells in the pore can be written in terms of the generating functions $A_i(x)$, $B_i(x)$ and $C_i(x)$ for the corresponding probabilities defined by Eqs. (4)-(6) as,

$$G(x) = [xp'_{N,1} + (1 - p'_{N,1})] A_{N-1}(x) + xp'_{N,0} B_{N-1}(x) + (1 - p'_{N,0}) C_{N-1}(x) . \quad (7)$$

where the generating function $A_i(x)$ is defined as $A_i(x) = \sum_{n=0}^i P_A(i, n)x^n$, while $B_i(x)$ and $C_i(x)$ are defined according to the same relation with A replaced by B and C , respectively.

Expressions for the generating functions $A_i(x)$, $B_i(x)$ and $C_i(x)$ for $i > 1$ can be found recursively in the following way. If cell $i - 1$ is occupied at the start of time-step $t = i$ and the local field at cell i is positive, i.e. $f_i = h_i + H > 0$, then cell i will become occupied during time-step $t = i$. This occurs with probability $p_{i,1}$, where

$$p_{i,m} = \int_{h=-H-J(2m-2)}^{\infty} \rho_{h_i}(h) dh . \quad (8)$$

If cell $i - 1$ is unoccupied then the random field has to be at a higher threshold $h_i > -H + 2J$ in order for cell i to become occupied during time-step i . The random field will be above this higher threshold with probability $p_{i,0}$, given by Eq. (8). If cell i does become occupied during time-step $t = i$ and $s_{i-1} = -1$ at this time, then an avalanche might pass back along the chain towards cell $i = 1$. This gives the expressions,

$$\begin{aligned} P_A(i, n') &= P_A(i - 1, n' - 1)p_{i,1} + P_B(i - 1, n' - 1)p_{i,0} , \\ P_C(i, n') &= P_A(i - 1, n')(1 - p_{i,1}) + P_C(i - 1, n')(1 - p_{i,0}) . \end{aligned} \quad (9)$$

If cell i does not become occupied at time step $t = i$, but cell $i + 1$ becomes occupied at some later time-step t' ($i < t' \leq N$) then cell i can also become occupied during time-step t' . The probability of cell i becoming occupied in this way at time step t' depends upon whether cell $i - 1$ is occupied or not. In fact, if cell $i - 1$ is occupied then cell i becomes occupied when cell $i + 1$ becomes occupied only if the random field at cell i is in the range $-H < h_i < -H + 2J$, which occurs with probability $p_{i,2} - p_{i,1}$. On the other hand, if cell $i - 1$ is unoccupied then the random field must be in the range $-H - 2J < h_i < -H$ in order for cell i to become occupied when cell $i + 1$ becomes occupied, which occurs with probability $p_{i,1} - p_{i,0}$. In the case that cell $i - 1$ is unoccupied, an avalanche of spin flips can propagate back down the chain from cell i towards cell 1 during time step t' . This gives the expression,

$$\begin{aligned} P_B(i, n') &= P_A(i - 1, n')(1 - p_{i,2}) + P_A(i - 1, n' - 1)(p_{i,2} - p_{i,1}) \\ &\quad + P_C(i - 1, n')(1 - p_{i,1}) + P_B(i - 1, n' - 1)(p_{i,1} - p_{i,0}) . \end{aligned} \quad (10)$$

Eqs. (9) and (10) lead to the following recursive relations for the generating functions, $A_i(x)$, $B_i(x)$ and $C_i(x)$,

$$\begin{aligned} A_i(x) &= x [A_{i-1}(x)p_{i,1} + B_{i-1}(x)p_{i,0}] \\ B_i(x) &= x(p_{i,2} - p_{i,1})A_{i-1}(x) + (1 - p_{i,2})A_{i-1}(x) + x(p_{i,1} - p_{i,0})B_{i-1}(x) + (1 - p_{i,1})C_{i-1}(x) \\ C_i(x) &= (1 - p_{i,1})A_{i-1}(x) + (1 - p_{i,0})C_{i-1}(x) , \end{aligned} \quad (11)$$

valid for $i > 1$.

The boundary values of $P_A(1, n')$ and $P_C(1, n')$ can be found using the following relations,

$$\begin{aligned} P_A(1, n') &= \delta_{n',1} p'_{1,0} , \\ P_C(1, n') &= \delta_{n',0} (1 - p'_{1,0}) , \end{aligned} \quad (12)$$

where $p'_{1,0}$ is the probability that cell 1 has a positive field (and thus becomes occupied) at the first time step (when all other cells are unoccupied). The value of $P_B(1, n')$ is given by the relation,

$$P_B(1, n') = (1 - p'_{1,1}) \delta_{n',0} + (p'_{1,1} - p'_{1,0}) \delta_{n',1} , \quad (13)$$

where $p'_{1,1} - p'_{1,0}$ is the probability that cell 1 has a negative local field during time-step $t = 1$, but the field becomes positive when cell 2 becomes occupied, and $1 - p'_{1,1}$ is the probability that cell 1 still has a negative local field after cell 2 becomes occupied. Eqs. (12) and (13) result in the following expression for the boundary generating functions,

$$\begin{aligned} A_1(x) &= x p'_{1,0} , \\ B_1(x) &= x (p'_{1,1} - p'_{1,0}) + 1 - p'_{1,1} , \\ C_1(x) &= 1 - p'_{1,0} . \end{aligned} \quad (14)$$

The generating function given by Eqs. (7), (11) and (14) can be written as a matrix equation,

$$G(x) = [\mathbf{A}(x)]^T \mathbf{M}_{N-1}(x) \mathbf{M}_{N-2}(x) \dots \mathbf{M}_2(x) [\mathbf{B}(x)] , \quad (15)$$

where,

$$\begin{aligned} [\mathbf{A}(x)]^T &= \left(x p'_{N,1} + (1 - p'_{N,1}), x p'_{N,0}, 1 - p'_{N,0} \right) , \\ \mathbf{M}_i(x) &= \begin{pmatrix} x p_{i,1} & x p_{i,0} & 0 \\ x(p_{i,2} - p_{i,1}) + (1 - p_{i,2}) & x(p_{i,1} - p_{i,0}) & 1 - p_{i,1} \\ 1 - p_{i,1} & 0 & 1 - p_{i,0} \end{pmatrix} , \text{ for } 1 < i < N , \\ [\mathbf{B}(x)]^T &= \left(x p'_{1,0}, x(p'_{1,1} - p'_{1,0}) + 1 - p'_{1,1}, 1 - p'_{1,0} \right) . \end{aligned} \quad (16)$$

Eqs. (15) and (16) are the expressions quoted in the main text.

-
- [1] J. P. Sethna, K. Dahmen, S. Kartha, J. A. Krumhansl, B. W. Roberts, and J. D. Shore, Phys. Rev. Lett. **70**, 3347 (May 1993), <http://link.aps.org/doi/10.1103/PhysRevLett.70.3347>
- [2] D. Dhar, P. Shukla, and J. P. Sethna, Journal of Physics A: Mathematical and General **30**, 5259 (1997), <http://stacks.iop.org/0305-4470/30/i=15/a=013>